Ray-Tracing for Mobile Communications

Sandra Knörzer, Thomas Fügen, and Werner Wiesbeck
Institut für Höchstfrequenztechnik und Elektronik (IHE), Universität Karlsruhe (TH)
Kaiserstr. 12, 76313 Karlsruhe, Germany, Phone: +49-721-608-2525
E-mail: Sandra.Knoerzer@ihe.uka.de

***Abstract*— For the parametrization and standardization of future mobile communications systems realistic values of the characteristic channel parameters are needed. Due to its ability to analyze the frequency-selective, time-variant as well as spatial behavior of the channel, ray-tracing is a popular channel characterization method. Moreover, it is capable to calculate very large structures (i.e. site-specific scenarios) with reasonable computation resources. In this paper three examples for ray-tracing for mobile communications are given after an introduction to the characteristic channel parameters. The advantages and challenges of this technique are described.**

I. Introduction

Wireless mobile communications in various applications is widespread and in different forms available everywhere. The term mobile covers diverse meanings, e.g. pedestrian-to-basestation, vehicle-to-basestation, car-to-car communications and many more. Communications is the generic term for information transportation from one place to another. This information can be as manifold as speech transmission, video screening, internet and multimedia applications, sensor and telemetric data. To provide all the different kinds of mobile communications a number of different systems and respective standards already exists and even more are still introduced. When setting up standards for new systems it is essential for the system designers to know the propagation channel for the desired application. Based on this, the system parameters like bandwidth, guard interval, subcarrier spacing etc. are chosen. But the knowledge of the channel is not only important for the design of new systems. It is furthermore relevant for existing systems and standards. E.g. if an already established system shall be used in a new environment or under special conditions not foreseen in the standard. Simulating the propagation channel with ray-tracing can verify the successful operation before installing the system and replace measurements to the largest part.
In this paper three application examples are given using a ray-tracing model developed at the IHE to characterize the channel parameters. First, the characteristic channel parameters for a high-speed train communications system are presented [1]. The fast moving trains cause high Doppler spread in the channel which is a special challenge for the design of the communications system. Second, the same ray-tracing tool is used to calculate the propagation channel in urban outdoor environments (base station to car) [2]. Third, a car-to-car communications system is modeled. The model is verified by comparing measurements with simulation results in a realistic urban scenario and in statistically generated highway scenarios [3].

II. Simulation using ray-tracing

Ray-tracing is based on a detailed simulation of the actual physical wave propagation process. In order to produce a deterministic description of the wave propagation, suitable formulations of the physical propagation phenomena are applied to a deterministically described scenario. The modeling of the propagation phenomena is usually based on geometrical optics (GO) and the uniform geometrical theory of diffraction (UTD). Ray-tracing describes each multi-path component found in a scenario by a ray. A distinction is made between different wave propagation phenomena by deriving several transmission paths. A detailed description of the propagation environment (size, position and composition of the material) is essential for an accurate channel prediction. For the ray-tracing technique it is assumed that all object dimensions in a scenario are larger than the wavelength (i.e. the frequency is high enough).
The examples presented in this paper are based on a 3D ray-tracing tool developed at the IHE. The propagation phenomena taken into account in this channel model are combinations of multiple reflections, multiple diffractions and diffuse scattering. The reflection of the rays is determined using the image theory and described with the modified Fresnel reflection coefficients. The diffraction uses Fermat's principle and the uniform geometrical theory of diffraction (UTD) [4]. The diffuse scattering is finally based on an obstructionless connection between the transmitter, the center of a Lambertian scattering surface and the receiver [5], [2]. Each ray path can consist of none, one or more interactions with objects in a scenario caused by the different propagation phenomena. The total propagation between a transmitter and a receiver is defined by all propagation paths. Therefore, the output of the ray-tracing procedure is a set of parameters for each identified propagation path in a snapshot: the complex transmission factor, the Doppler shift f_{D}, the time delay of arrival (TDA) τ, the direction of departure (DoD) and the direction of arrival (DoA) each in azimuth ψ and elevation θ.
For mobile environments sets of consecutive snapshots are simulated. The mobility of the scenario is modeled by allocating the appropriate velocities and changing the object positions (e.g. a moving vehicle hosting a mobile receiver is situated in different locations according to its trajectory and different antenna positions).

III. Channel characteristics

For the optimization of existing and for the design of new wireless communications systems, it is essential to take the propagation characteristics of the operating environment into account. The ray-tracing model described in Section II is particularly suitable as it distinguishes inherently between different discrete propagation paths. It is therefore possible to easily estimate the narrow- and wide-band as well as the spatial channel characteristics. Analyzing the narrow-band transmission channel, the parameters describing the time variance are obtained. This means that the variation of the frequency response at a single frequency is examined. The parameters describing the frequency selectivity are obtained by analyzing the channel over the complete bandwidth of the system. The following description is limited to a short definition of the equivalent low-pass frequency response with a description of the long-term and short-term fading as well as the channel parameters as they are used for the evaluation of ray-tracing results. The ray-tracing results are theoretically valid for infinite bandwidth as given in the following formulas. For the comparisons to measurements the respective system bandwidth has to be introduced [2].

A. Time-variance (narrow-band description)

The equivalent low-pass frequency response is defined as

$$H^{\mathrm{LP}}(\nu,t) = \sum_{n=1}^{N(t)} A_n(t)\cdot e^{-j2\pi(f_c+\nu)\tau_n(t)} \quad (1)$$

With $A_n(t)$ being the complex amplitude of the n^{th} path at time instant t, N being the total number of paths for this instant, f_c the center frequency, $\nu = f - f_c$ the frequency shift versus the center frequency and $\tau_n(t)$ the delay time of each path. As in ray-tracing simulations the time t is not given continuously but in discrete snapshots the parameter is called t_{d} in the following. The transmission factor $\left|H^{\mathrm{LP}}(t_{\mathrm{d}})\right|$ consists of a fast and a slowly fluctuating component (2), the short-term and the long-term fading, respectively. Averaged over an appropriate even number of consecutive snapshots K the transmission factor reveals the long-term fading $l(t_{\mathrm{d}})$ (3). Reasonable numbers of snapshots reflect movement in the scenario between 40 λ and 200 λ [6].

$$\left|H^{\mathrm{LP}}(t_{\mathrm{d}})\right| = l(t_{\mathrm{d}})s(t_{\mathrm{d}}) \quad (2)$$

$$l(t_{\mathrm{d}}) = \frac{\sum_{k=d-(K-1)/2}^{d+(K-1)/2}\left|H^{\mathrm{LP}}(t_{\mathrm{k}})\right|}{K} \quad (3)$$

The long-term characteristics of a channel are usually given by a path loss curve versus simulation or measurement time. The short-term fading $s(t_{\mathrm{d}})$ is calculated by the transmission factor divided through the according value for the long-term fading.

$$s(t_{\mathrm{d}}) = \frac{\left|H^{\mathrm{LP}}(t_{\mathrm{d}})\right|}{l(t_{\mathrm{d}})} \quad (4)$$

From these functions versus simulation or measurement time important statistical curves can be derived. E.g. the cumulative distribution function (CDF) characterizes the cumulated probability that the amplitude of the short-term fading signal is lower than the value on the abscissa. More definitions like the level crossing rate or the average fade duration can be found in [6].

Each ray within one snapshot suffers from a corresponding Doppler shift. The Doppler behavior within one snapshot can be characterized by the Doppler spectrum which shows the power density versus Doppler frequency. From the Doppler spectrum two characteristic values are derived: the mean Doppler shift and the Doppler spread. The expectation value of the Doppler shift is called mean Doppler shift and can be directly calculated from the ray-tracing results by

$$\mu_{f_{\mathrm{D}}} = \frac{\sum_{n=1}^{N} f_{\mathrm{D,n}}\left|A_n\right|^2}{\sum_{n=1}^{N}\left|A_n\right|^2} \quad (5)$$

With N being the number of paths in the relevant snapshot and A_n the complex amplitude of the n^{th} path. The variance of the Doppler shift weighted by the power (Doppler spread) is

$$\sigma_{f_{\mathrm{D}}} = 2\sqrt{\frac{\sum_{n=1}^{N} f_{\mathrm{D,n}}^2\left|A_n\right|^2}{\sum_{n=1}^{N}\left|A_n\right|^2} - {\mu_{f_{\mathrm{D}}}}^2} \quad (6)$$

For a total of M consecutive snapshots the time-average mean Doppler shift is

$$\overline{\mu_{f_{\mathrm{D}}}} = \frac{\sum_{m=1}^{M}\mu_{f_{\mathrm{D}},m}}{M} \quad (7)$$

and the time-average Doppler spread

$$\overline{\sigma_{f_{\mathrm{D}}}} = \frac{\sum_{m=1}^{M}\sigma_{f_{\mathrm{D}},m}}{M} \quad (8)$$

B. Frequency-selectivity (wide-band description)

The frequency-selective parameters are the wide-band description and reveal the properties of the channel considering time. Analog to the time-variant description with the Doppler spectrum the frequency selective behavior is represented by the Power Delay Profile (PDP) which shows the power density versus time delay. For one snapshot the mean delay which represents the expectation value can be determined by

$$\mu_{\tau} = \frac{\sum_{n=1}^{N}\tau_n\left|A_n\right|^2}{\sum_{n=1}^{N}\left|A_n\right|^2} \quad (9)$$

The variance of the time delay within one snapshot is given by the delay spread

$$\sigma_\tau = \sqrt{\frac{\sum_{n=1}^{N} \tau_n^2 |A_n|^2}{\sum_{n=1}^{N} |A_n|^2} - {\mu_\tau}^2} \quad (10)$$

For a series of M consecutive snapshots the time-average mean delay is calculated by

$$\overline{\mu_\tau} = \frac{\sum_{m=1}^{M} \mu_{\tau,m}}{M} \quad (11)$$

and the time-average delay spread, respectively

$$\overline{\sigma_\tau} = \frac{\sum_{m=1}^{M} \sigma_{\tau,m}}{M} \quad (12)$$

C. Angular-dispersion (spatial description)

Analog to the time and frequency domain there are the Angular Power Spectrum (APS) and characteristic parameters to express the angular dispersion in the channel. The parameters exist for the transmit as well as the receive side in azimuth and elevation. Only one combination each is representatively given here. Even though the ray-tracing results yield discrete angular information for each path we can not simplify the integral in the following equations to a sum. This is due to the unequal angular stepwidth. First, the mean azimuth angle for the transmitter (T) is [2]

$$\mu_{\psi_\mathrm{T}} = \frac{\int_{\psi_{\mathrm{T,max}}-\pi}^{\psi_{\mathrm{T,max}}+\pi} \psi_\mathrm{T} |A(\psi_\mathrm{T})|^2 \, d\psi_\mathrm{T}}{\int_{\psi_{\mathrm{T,max}}-\pi}^{\psi_{\mathrm{T,max}}+\pi} |A(\psi_\mathrm{T})|^2 \, d\psi_\mathrm{T}} \quad (13)$$

With with the power maximum being at the azimuth angle $\psi_{\mathrm{T,max}}$. The variance is called angular spread

$$\sigma_{\psi_\mathrm{T}} = \sqrt{\frac{\int_{\psi_{\mathrm{T,max}}-\pi}^{\psi_{\mathrm{T,max}}+\pi} \psi_\mathrm{T}^2 |A(\psi_\mathrm{T})|^2 \, d\psi_\mathrm{T}}{\int_{\psi_{\mathrm{T,max}}-\pi}^{\psi_{\mathrm{T,max}}+\pi} |A(\psi_\mathrm{T})|^2 \, d\psi_\mathrm{T}} - \mu_{\psi_\mathrm{T}}^2} \quad (14)$$

For a set of M snapshots the time-average mean azimuth angle is calculated by

$$\overline{\mu_{\psi_\mathrm{T}}} = \frac{\sum_{m=1}^{M} \mu_{\psi_\mathrm{T},m}}{M} \quad (15)$$

and the time-average angular spread

$$\overline{\sigma_{\psi_\mathrm{T}}} = \frac{\sum_{m=1}^{M} \sigma_{\psi_\mathrm{T},m}}{M} \quad (16)$$

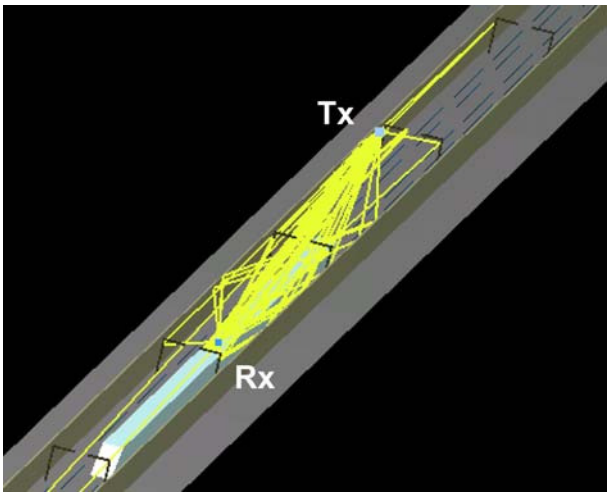

Fig. 1. High-speed train in a noise barrier scenario. The yellow lines represent the simulated propagation rays.

IV. Base station to train communications

The first example for the application of ray-tracing in mobile communications is a wireless communications system for high-speed trains [1]. The channel model includes a 800 m long train track with metallic tracks and pylons supported by a concrete track bed. On both sides of the track are concrete noise barriers. A high-speed train consisting of metal moves through the scenario with a velocity of 111 m/s. An omnidirectional transmit antenna (Tx) is situated at the track side and an omnidirectional receive antenna (Rx) on top in the middle of the train. Both antennas are vertically polarized. Resulting from the ray-tracing simulation the propagation paths in the scenario are determined and the characteristic parameters can be calculated. Fig. 1 shows a segment of the simulated train track with the resulting ray paths displayed as yellow lines. Fig. 2 shows the receive power of each path

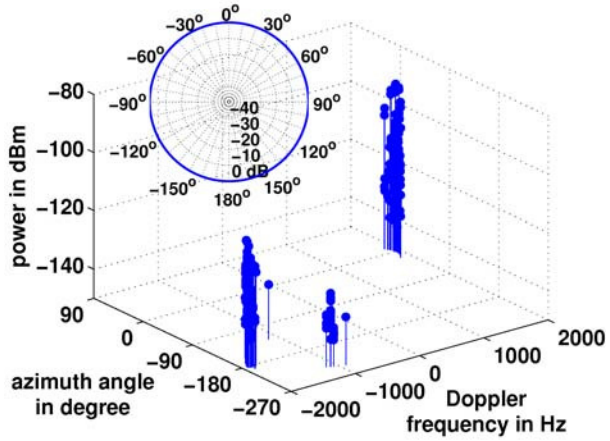

Fig. 2. Path power versus Doppler frequency and azimuth angle (DoA) for a representative snapshot using an omnidirectional train antenna (azimuth pattern given in the upper left-hand corner)

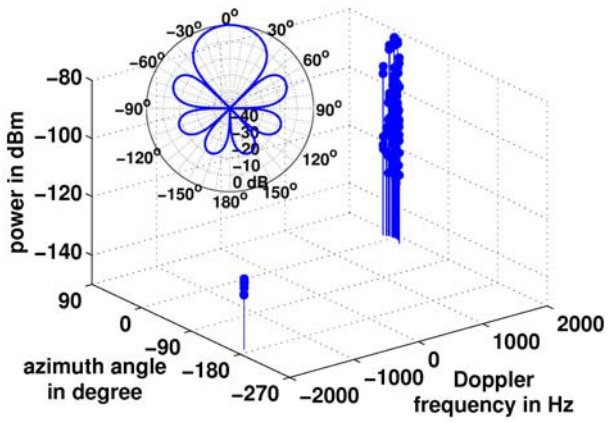

Fig. 3. Path power versus Doppler frequency and azimuth angle (DoA) for a representative snapshot using a directional train antenna (azimuth pattern given in the upper left-hand corner)

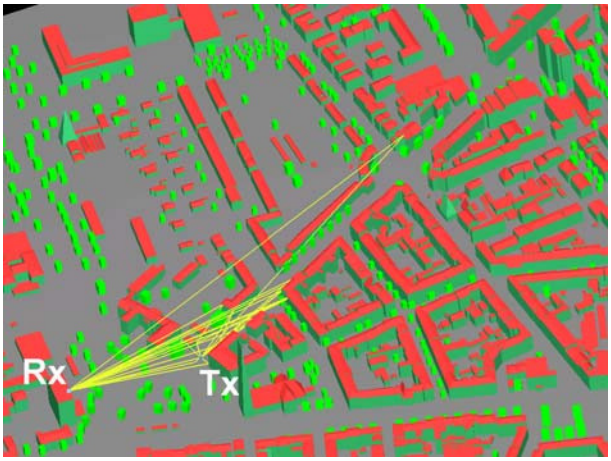

Fig. 4. Base station to car communications scenario

versus the azimuth angle (DoA) and the Doppler frequency of the paths. The azimuth angle $\psi = 0°$ points into the direction of movement of the train, i.e. angles in this region are pointing in the direction of the transmitter. The antenna pattern shown in the upper left-hand corner indicates the azimuth pattern of the omnidirectional antenna. When looking at the azimuth distribution of the representative snapshot it is obvious that paths arrive only from selected angular ranges, mainly from the angular range around $0°$ and $-180°$. The Doppler frequency values correlate with the azimuth angles. The Doppler spread for this snapshot is $\sigma_{f_\mathrm{D}} = 1425.7\,\mathrm{Hz}$ and the azimuth spread at the receiver on top of the train $\sigma_{\psi_\mathrm{R}} = 33.9°$. In a wireless communications system a lower Doppler spread value (assuming the same signal-to-noise ratio) stands for lower bit error rate or higher data rate. To decrease the Doppler spread value in this channel a directive train antenna is used. Fig. 3 shows the same simulation as in Fig. 2 but using a directional antenna. The relevant directional antenna azimuth pattern is given in the upper left-hand corner of the figure. The difference compared to the previous case is that the paths impinging on the receiver from the $-180°$ range are attenuated or have completely vanished whereas the paths from the $0°$ range are amplified due to the pattern. The azimuth spread shrinks to $\sigma_{\psi_\mathrm{R}} = 6.0°$. This results also in a reduced Doppler spread of $\sigma_{f_\mathrm{D}} = 45.8\,\mathrm{Hz}$. The 3D ray-tracing tool and its visualization of the wave propagation helps to identify the spatial characteristics which directly influence the Doppler spread.

V. Base station to car communications

Concerning the popular application of a base station to car communications the scenario in Fig. 4 is considered. The base station (Rx) is mounted on top of a tall building at a height of $40\,\mathrm{m}$. The mobile station (Tx) is moving at a speed of $v = 7.3\,\mathrm{km/h}$ along a straight route. The antenna at the mobile station is mounted at the height of $2.1\,\mathrm{m}$ with an operating frequency of $5.2\,\mathrm{GHz}$. In Fig. 4 the yellow lines resemble the strongest multi-path components. Several reflections and diffractions occur at the buildings in the vicinity of the transmitter, which is typical for urban macrocellular environments. Diffuse scattering from trees contributes to the received signal as well. For illustration reasons, scattering is not visualized in this example. At the transmitter a vertically polarized monocone antenna and at the receiver a vertically polarized $\frac{\lambda}{4}-$antenna are used. The normalized received power is modeled by the ray-tracing tool. To verify the results of the tool measurements are performed and compared with the simulation results [2]. Fig. 5 shows a comparison of the measured and simulated long-term fading received power. With increasing time the separation of the base and mobile station increases. Therefore, the received power drops down. Most of the measured characteristics are found also in the simulation. The mean error is $\mu = 1.27\,\mathrm{dB}$, and the standard deviation is $\sigma = 2.85\,\mathrm{dB}$, which shows a very good agreement between measurement and simulation. The short-term fading adds up

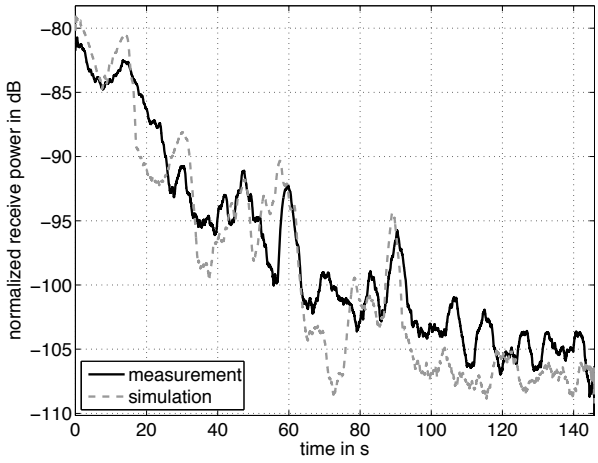

Fig. 5. Long-term fading

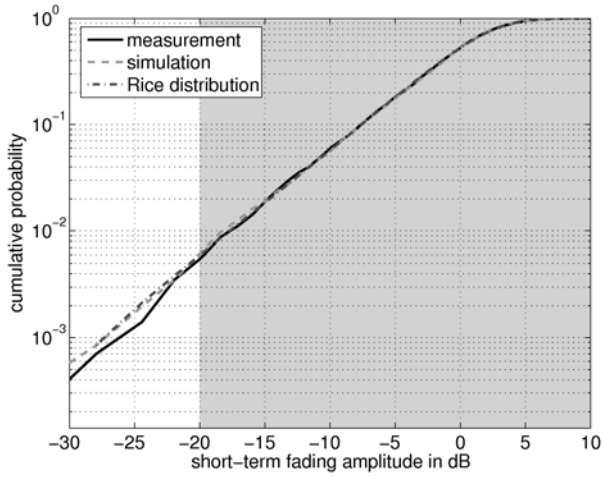

Fig. 6. Cumulative distribution function (CDF) of the short-term fading

to the long-term fading shown in Fig. 5. In order to evaluate the ability of the ray-tracing tool to describe short-term fading the cumulative distribution function is regarded in Fig. 6. There is a significant deviation of the simulated and measured short-term fading for very small fading amplitudes. Over the whole range depicted in Fig. 6 the maximum difference equals 200 %, the mean difference equals 20.7 %. Regarding only fading amplitudes larger than $-20\,\mathrm{dB}$ (shaded region in Fig. 6) the graph shows a much smaller difference of just 14.2 % for the maximum difference and 4.3 % for the mean difference, respectively. Therefore, the ray-tracing tool allows a very good description of the short-term fading characteristics for fading amplitudes larger than $-20\,\mathrm{dB}$. For very small amplitudes large deviations exist. This means significant short-term fading contributions can be modeled with good accuracy.

VI. Car-to-car communications

In the last example, again the direct comparison of measurement and simulation data is given. Fig. 7 shows the measurement conditions (a) and the simulation setup (b). A transmit (Tx) and a receive (Rx) antenna, both vertically polarized, are positioned on two vans driving along a motorway with line-of-sight (LOS) condition. At the roadsides there is vegetation. The traffic flow in the simulation is statistically generated except the transmitter and receiver van as well as the truck driving in front of both vans. The 3D ray-tracing tool is used to simulate the wave propagation in this environment. The PDP of both, the measurement and simulation, is given in Fig. 8. Different objects can be identified as origin for the occurring lines. The lowest horizontal line extending over the whole considered time represents the LOS path. Parallel to the LOS path another line is found which is caused by the truck driving constantly in front of the transmitter and receiver van. Ascending and descending lines originate from either non-moving objects or vehicles with a velocity different from the transmitter and receiver. The object velocity can be derived from the slope of the lines. The lines do not fit quantitatively

(a)

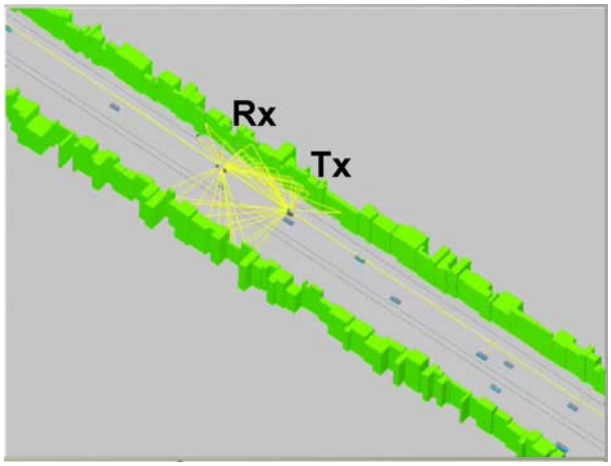

(b)

Fig. 7. Car-to-car communications in a motorway scenario (picture of measurement (a) and ray-tracing simulation (b))

because the traffic scenario for the simulation is modeled statistically. Nevertheless, there is a very good agreement of the qualitative outcome of measurement and simulation. This is due to a very realistic traffic model, in which the movement of each car, i.e. its position in the calculated snapshots and the allocated velocity, is modeled according to the given traffic density and traffic flow.

VII. Conclusion

In this paper three examples for 3D ray-tracing simulations for mobile communications are given. Partly they are compared to and verified by measurements. In general simulation and measurement show good or even excellent agreement of the full narrow-band and wide-band mobile transmission channel. The quality of the simulation strongly depends on the quality of the traffic model and the realistic environment. On the one hand, the required high quality of the traffic model and environment data results in higher implementation and calculation effort compared to simple wave propagation models. On the other hand, ray-tracing yields very good

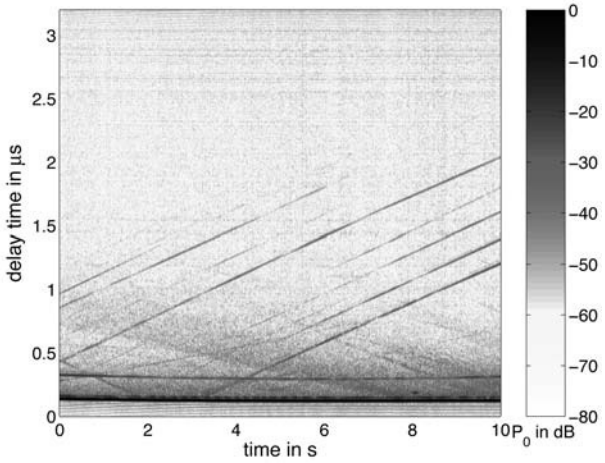

(a)

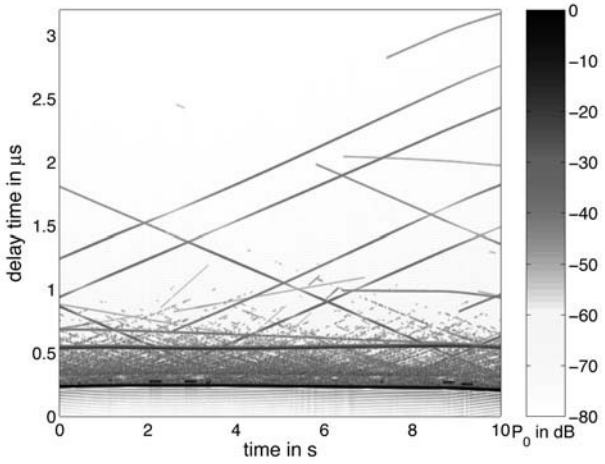

(b)

Fig. 8. Power delay profile for car-to-car communications in a motorway environment: measurement (a) and ray-tracing simulation (b)

agreement of the full narrow-band and wide-band channel information.

The calculation time and memory requirements are manageable for up-to-date computers and considering the large scenario dimensions very efficient. For the wave propagation modeling in a specific scenario, ray-tracing strikes a balance between the fast but inaccurate simple models and the full-wave analysis which is very exact but limited to small scenarios. Moreover, one of the main advantages of ray-tracing is that it yields the complete channel information in time, frequency and space.

Therefore, ray-tracing is an adequate tool for setting up new system standards as well as feasibility studies in wireless mobile communications or for testing existing systems on their operability in unforeseen and difficult environments. Future wireless systems may be either base station to mobile (e.g. cars, trucks, trains, pedestrians) or vehicle to vehicle communications which can both be handled by ray-tracing. Ray-tracing simulations can replace measurements only to a certain extend but never completely. Measurements should be used in addition to simulations; at least they are needed for the verification.

REFERENCES

[1] S. Knörzer, M. A. Baldauf, T. Fügen, and W. Wiesbeck, "Channel Modelling for an OFDM Train Communications System Including Different Antenna Types," *IEEE 64th Vehicular Technology Conference*, September 2006, CD-ROM.

[2] T. Fügen, J. Maurer, T. Kayser, and W. Wiesbeck, "Capability of 3-D ray tracing for defining parameter sets for the specification of future mobile communications systems," *IEEE Transactions on Antennas and Propagation*, vol. 54, no. 11, pp. 3125–3137, Nov 2006.

[3] J. Maurer, T. Fügen, and W. Wiesbeck, *Proceedings in Physics: Fields, Networks, Computational Methods, and Systems in Modern Electrodynamics*, chapter A Ray-Optical Channel Model for Vehicle-to-Vehicle Communication, pp. 243–254, Springer, Berlin, Dec 2004.

[4] R.J. Luebbers, "Comparison of lossy wedge diffraction coefficients with application to mixed path propagation loss prediction," *IEEE Transactions on Antennas and Propagation*, vol. 36, no. 7, pp. 1031–1034, July 1998.

[5] J. Maurer, S. Knörzer, and W. Wiesbeck, "Ray tracing in rich scattering environments for mobile-to-mobile links," *International Conference on Electromagnetics in Advanced Applications*, pp. 1073–1076, Sept. 2005.

[6] W.C.Y. Lee, *Mobile communications engineering*, McGraw-Hill, 1982.